HEAT RECOVERY FROM A NATURAL GAS POWERED INTERNAL COMBUSTION ENGINE BY CO_2 TRANSCRITICAL POWER CYCLE

by

Mahmood FARZANEH-GORD* *, Seyed Aliakbar MIRMOHAMMADI, Mohammadreza BEHI, and Amin YAHYAIE

Faculty of Mechanical Engineering, Shahrood University of Technology, Shahrood, Iran

Original scientific paper
UDC: 621.412.43:622.324.6
DOI: 10.2298/TSCI1004897F

The present work provides details of energy accounting of a natural gas powered internal combustion engine and achievable work of a utilized CO_2 power cycle. Based on experimental performance analysis of a new designed IKCO (Iran Khodro Company) 1.7 litre natural gas powered engine, full energy accounting of the engine were carried out on various engine speeds and loads. Further, various CO_2 transcritical power cycle configurations have been appointed to take advantages of exhaust and coolant water heat lost. Based on thermodynamic analysis, the amount of recoverable work obtainable by CO_2 transcritical power cycles have been calculated on various engine conditions. The results show that as much as 18 kW power could be generated by the power cycle. This would be considerable amount of power especially if compared with the engine brake power.

Key words: *internal combustion engine, energy analysis, CO_2 power cycle, exhaust heat recovery*

Introduction

There have been a numerous researches on energy conservation and its efficient use in recent years. The current reduction in oil reserves combined with the increase in its price, as well as the need for cleaner fuels, have led in the past years to an increasing interest and research in the field of waste heat recovery [1, 2].

Perhaps, the best known engines in world for generating mobile power are the reciprocating internal combustion engines (ICE). It is well known that majority of fuel energy in a typical engine are wasted through exhaust gases and cooling water radiator. These make exhaust and cooling water heat recovery is matter of necessary in current world energy situation.

Various methods have been proposed to recover energy from an ICE waste heat to produce power or refrigeration. One of the attractive waste energy recovery methods is CO_2 gas power cycle. The method has the potentials to be implemented in a typical car to convert heat lost to usable work.

* Corresponding author; e-mail: m.farzanehgord@gmail.com

Research on the CO_2 power cycle began on 1948. As mentioned by Chen [3], after its prosperity in the 1960s, research on the cycle, however, dwindled for many years until the 1990s, mainly due to limited amount of suitable heat sources and limited knowledge in suitable compact heat exchangers and suitable expansion machines. After the 1990s and development of compact heat exchangers and materials, *etc*., renewed interest was shown in the CO_2 power cycle and much research has been carried out including work of Dostal *et al.* [4]. Nevertheless, most investigations have focused on a CO_2 power cycle with a nuclear reactor as a heat source, thus the cycle working with a high grade heat source (up to 800 °C) and high pressures in both the gas heater and gas cooler (CO_2 Brayton cycle). Chen [3] has proposed and analyzed three CO_2 novel cycles, namely: the CO_2 transcritical power cycle, the CO_2 Brayton cycle, and the CO_2 cooling and power combined cycle. The author concluded that due to the different characteristics of each cycle, the three cycles are suitable for different applications. The CO_2 transcritical power cycle is suitable for harvesting energy from low grade heat sources, near which a low temperature heat sink is accessible. The CO_2 Brayton cycle is suitable for harvesting the energy from relatively high grade heat sources when there is no low temperature heat sink available. The CO_2 cooling and power combined cycle is suitable for applications, where both power and cooling are needed.

There have been researches on utilizing CO_2 cooling and power cycle on mobile application such as automobiles. The aims were to recover heat lost from engine exhaust to produce power and cooling. Chen *et al.* [5] have studied theoretically, new means to utilize the low-grade small-scale energy in vehicle exhaust gas and investigated several CO_2 basic cycle layouts according to the design concepts. Due to fact that the work obtained from the proposed cycle is all converted from the energy in the exhaust gas-even if the cycle achieve low cycle efficiency – it might still be interesting as long as the system proves to be cost effective. All the theoretical results demonstrate that the proposed idea is suitable for utilization of the energy in vehicle exhaust gas. Farzaneh-Gord *et al.* [6] simulated a CO_2 power cycle and calculated the amount of recoverable energy (work) from the exhaust of a typical passenger car. The calculation was based on the actual exhaust gas flow rate of a typical passenger car. Further, Farzaneh-Gord *et al.* [7] have appointed two possible CO_2 Brayton cycle configurations to take advantages of engine heat lost. Based on thermodynamic analysis, the amount of recoverable work, obtainable by CO_2 Brayton cycles have been calculated on various engine conditions and found to be as much as 17 kW.

For low-grade and high-grade heat sources, different working fluids have different results and performance. Considering the low-grade source energy of exhaust gas, carbon dioxide proved to be the most promising working fluid. Cayer *et al.* [8] have presented a detailed analysis of a carbon dioxide transcritical power cycle using an industrial low-grade stream of process gases as its heat source. They divide the methodology in four steps: energy analysis, exergy analysis, finite size thermodynamics and calculation of the heat exchangers' surface. Their results show the existence of an optimum high pressure for each of the four steps; in the first two steps, the optimum pressure maximises the thermal or exergetic efficiency while in the last two steps it minimises the product *UA* or the heat exchangers' surface.

There have been also researches on utilizing CO_2 as working fluid for automotive air conditioners using vapor compression cycle. Brown *et al.* [9] evaluated performance merits of CO_2 and R134a automotive air conditioning systems using semi-theoretical cycle models. They derived an equitable comparison of performance of those two working fluids where the components in both systems were equivalent and differences in thermodynamic and transport proper-

ties were accounted for in the simulations. The analysis showed R134a having a better COP than CO_2 with the COP disparity being dependent on compressor speed (system capacity) and ambient temperature.

There have been other proposed cycles for automotive air conditioners such as absorption refrigeration cycle. Ramanathan *et al.* [10] studied an absorption refrigeration system which was driven by the heat from the exhaust gases of a mid sized passenger car. They concluded that 2 kW of cooling could be provided for air conditioning at both idle and cruise speed conditions.

The performance analysis of an ICE was also an interested subject in research papers. Farzaneh-Gord *et al.* [11] have developed a computer program to simulate four stroke spark ignition engine. The simulation has been done considering intake and exhaust processes as well as compression and combustion processes. It studies the effects of different parameters on engine efficiency and proposed the optimized conditions for fuel octane. Evans *et al.* [12] carried out a comparison of simulation results with experimentally measured performance data in a lean-burn engine operating with natural gas over a wide range of air-fuel ratios. Recent studies show that almost 1/3 of the energy of a fossil fuel is destroyed during the combustion process in power generation including work of Stone [13]. This has caused a renewed interest in availability analyses, since effective management and optimization of thermal systems is emerging as a major modern technical problem. Rakopolus *et al.* [14] have carried out a method for the second law analysis of the internal combustion engines operation with dodecane fuel and use it to analyze the operation with alternative fuels. Sobiesiak *et al.* [15] used first and second law of thermodynamic to analyze engine performance and optimize design of spark ignition (SI) engines fuelled with compressed natural gas (CNG).

The present work expands considerably upon those papers, providing details about energy accounting of a natural gas powered ICE and achievable work of a utilized CO_2 power cycle. Based on experimental performance analysis of a new designed IKCO (Iran Khodro Company) 1.7 liter natural gas powered ICE, full energy accounting of the engine was carried out on various engine speeds and loads. The energy accounting includes (a) exhaust gases analysis, its temperature and mass flow rate, (b) coolant inlet and outlet temperature and its mass flow rate and (c) the engine brake power and torque. Further, various CO_2 transcritical power cycle configurations have been appointed to take advantages of exhaust and coolant water heat lost. Based on thermodynamic analysis, the amount of recoverable work obtainable by CO_2 transcritical power cycles have been calculated on various engine conditions.

Energy accounting of natural gas powered 1.7-litre engine manufactured at IKCO

IKCO has unveiled the first national (Iranian) natural gas powered engine family in 2005 known as EF7 family. The engines were developed jointly by Iran Khodro Powertrain Company and German FEV Motorentechnik GmbH. The one which has been studied here is 1.7 liter natural aspirated spark ignition engine. The details of the engine parameters are given in tab. 1. The engine is capable of consuming natural gas or gasoline as fuel. However the experimental values which presented here are based on natural gas as fuel. Table 2 shows the fuel properties which consumed during engine tests.

Figure 1 shows a schematic diagram of the experimental apparatus and measuring devices. It should be pointed out that the tests have been carried out by IKCO. As it can be seen in

Table 1. 1.7 liter natural gas power EF7 IKCO engine basic parameters

Parameter	Value	Unit
Type	Spark ignited	
Charging method	Natural aspirated	
Cylinder number	4	
Bore	78.6	mm
Stroke	85	mm
Displacement	1646	cm^3
Compression ratio	11.05	
Max. power	80	kW
Speed at max. power	6000	rpm
Max. torque	136	Nm
Speed at max. torque:	3500	rpm
Idle speed	750	rpm
Valve number of each cylinder	4	
Angle of air valve opening	Variable	deg
Angle of air valve closing	Variable	deg
Angle of exhaust valve opening	17	deg
Angle of exhaust valve closing	9	deg

Table 2. Natural gas fuel properties consumed during engine test

Parameter	Value	Unit
Heating value (LHV)	45.47	MJ/kg
Fuel composition		
– CH_4	87.0	Vol. fraction
– C_2H_6	5.0	Vol. fraction
– C_3H_8	2.0	Vol. fraction
– N_2	6.0	Vol. fraction
Molecular weight	18.31	g/mol
Stoichiometric air requirement	15.58	–

the figure, the fuel, air and coolant flow rates are measured by appropriate flow meters. Exhaust gas temperature are measured with 4 thermometers in each exhaust runner. The exhaust temperature is calculated by averaging these values. Inlet and outlet coolant temperature are measured by two thermometers. Engine power is measured by measuring engine speed and the engine torque using a dynamometer.

Figure 2 shows exhaust gases temperature on full and half loads for various engine speeds. It can be realized that as the engine speed increases, the exhaust gases temperature increases too.

Knowing, exhaust mass flow rate, $\dot{m}_{ex}$, exhaust gases temperature T_{ex}, and ambient temperature T_0, one can calculate exhaust heat lost as:

$$\dot{Q}_{ex} \quad \dot{m}_{ex} c_{p,mix} (T_{ex} \quad T_0) \quad (1)$$

It is well know that coolant heat lost is other main source of energy lost in an engine. By measuring inlet and outlet coolant temperatures and coolant mass flow rate, one can calculate the coolant heat lost as:

$$\dot{Q}_w \quad \dot{m}_w c_{p,w} (T_{wi} \quad T_{wo}) \quad (2)$$

Considering the engine as thermodynamic system, one can write overall heat balance for the engine as:

$$\dot{m}_f LHV \quad \dot{Q}_{ex} \quad \dot{Q}_w \quad \dot{Q}_{res} \quad \dot{W}_{ICE} \quad (3)$$

In eq. 3, $\dot{m}_f$ is the fuel mass flow rate, $\dot{m}_f LHV$ – the input fuel energy, $\dot{W}_{ICE}$ – the engine power, and $\dot{Q}_{res}$ – the rest of engine en-

ergy. $\dot{Q}_{res}$ includes heat lost from engine surface, consumed power by engine accessories, irreversibility in combustion process and other terms. This value ($\dot{Q}_{res}$) could not be measured and should be calculated using eq. 4. By dividing right side terms by input energy (fuel energy), the percentage of input energy consumed by each term could be calculated.

Figures 3 and 4 shows percentage of consumed energy of each term *vs.* engine speed for half and full load, respectively. It can be realized that, at lower engine speed, coolant water losses more energy than exhaust but at higher engine speed, it is exhaust gases which losses more energy. Rest term consumes more percentage of fuel energy at half load comparing to full load. Finally, the engine is more efficient in medium speed to generate power for both half and full load.

It can be also seen that, approximately, the coolant and exhaust heat lost are destroyed 60% of input fuel energy during engine operation. So it can be concluded that any action which could recover the heat lost, will improve overall efficiency of the engine significantly. Further, this exposes possibility of utilizing low grade heat source power cycle such as a CO_2 transcritical power cycle.

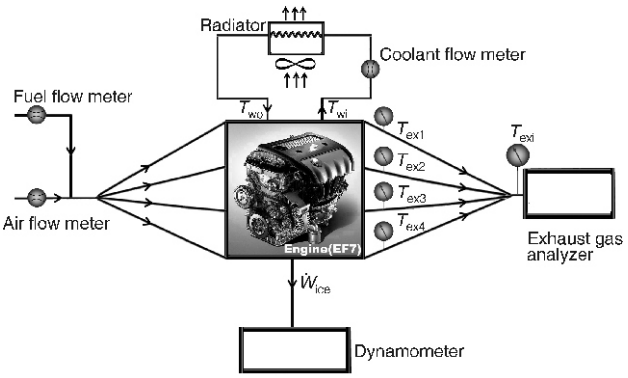

Figure 1. A schematic diagram of experimental lay-out

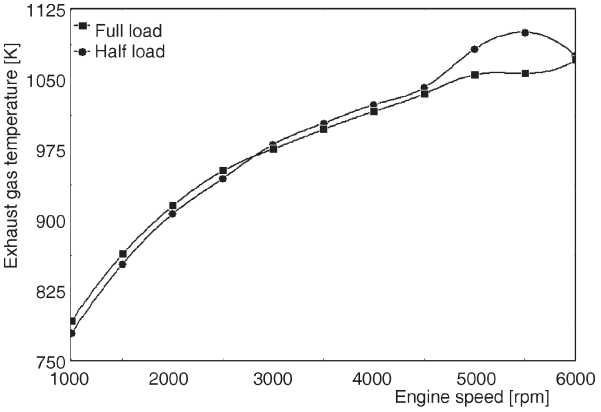

Figure 2. The exhaust gas temperature at full and half load for various engine speeds

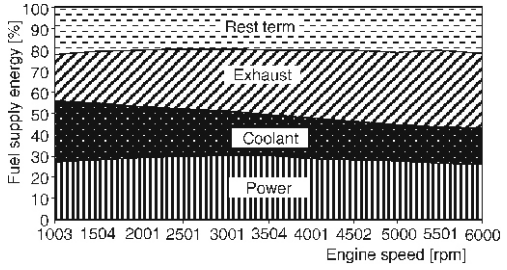

Figure 3. The percentage of energy consumed by each term at half load for various engine speeds

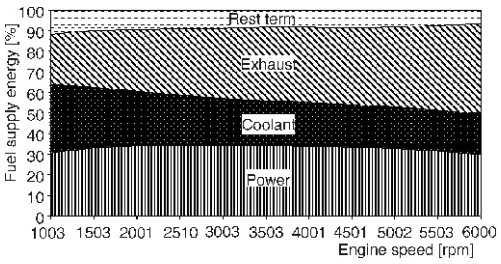

Figure 4. The percentage of energy consumed by each term at full load for various engine speeds

The proposed heat recovery systems

As mentioned in previous section, there is a good potential to utilize heat recovery power cycle to take advantage of heat lost from the ICE. As proposed by previous researchers such as Chen *et al.* [5], the CO_2 power cycle is suitable for recovering heat lost of a vehicle exhaust gases. So, in this study, the CO_2 transcritical power cycle has been selected to take advantage of the engine heat lost. Considering the facts that there are two main heat sources from the engine, there are possibilities to take advantage of one or both heat sources. There is also possibility of employing internal heat exchanger in the power cycle. This makes totally 4 possible configurations (It should be noted that the gas heat source should be existed in any configurations). These configurations are as shown in fig. 5 to 8. In this study, all of these configurations have been studied. The aim is to generate net power as much as possible. The configurations are abbreviated as GHC (gas heat source cycle), GWHC (gas and water hear sources cycle), GHIC (gas heat source with internal heat exchanger cycle), and GWHIC (gas and water heat sources with internal heat exchanger cycle).

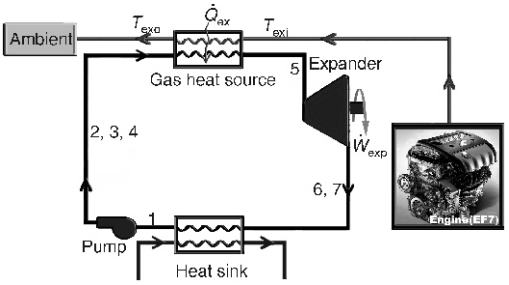

Figure 5. The configuration with gas heat source only (GHC)

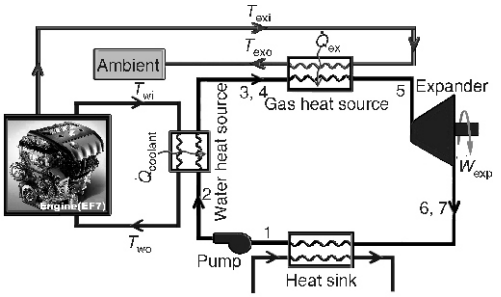

Figure 6. The configuration with gas and water heat sources (GWHC)

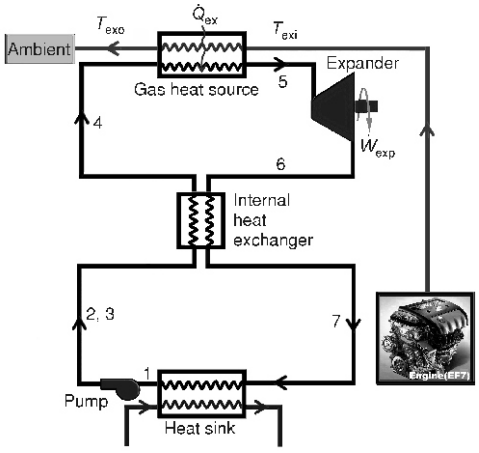

Figure 7. The configuration with gas heat source and internal heat exchanger (GHIC)

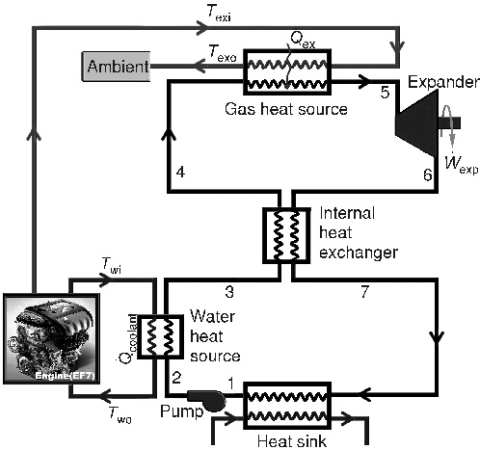

Figure 8. The configuration with gas and water heat sources and internal heat exchanger (GWHIC)

System modelling

Modelling assumptions

There have been some researches on CO_2 transcritical power cycle in low grade heat source recovery applications. In this study based on these researches especially work of Cayer *et al.* [8] and Chen *et al.* [5], the following assumptions have been made to specify the cycles working conditions. The steady-state steady flow has been assumed in all components, the kinetic and potential energies as well as the heat and friction losses are neglected, the pump and the expander turbine isentropic efficiency set at 0.8. The condenser pressure is set to 60 bar with the corresponding condensing temperature at 22 °C. The gas heat source pressure is varied from 120 bar depends to gas heat source to condenser pressure ratio (β). A temperature difference of 15 °C are assumed at inlet and outlet of gas and water heat sources between hot stream (exhaust gases or coolant) and cold stream (CO_2 stream). For case of existence of an internal heat exchanger, the internal heat exchanger effectiveness is assumed to be 0.7.

The analysis has been carried out using EES (engineering equation solver) software and built in properties data. Coolant water assumed to be pure water with constant specific heat. The specific heat for exhaust gases has been assumed constant and calculated using eq. 2 at the average gas heater temperature.

Calculation procedure

The first law of thermodynamics has been employed to analysis the cycles. Considering fig. 8, the following procedure has been carried out to perform the analysis for GWHIC configuration. The procedure for other configuration demands less effort.

Knowing inlet and outlet pump pressure and isentropic efficiency, the outlet enthalpy and temperature of the pump could be calculated by employing the equation:

$$h_2 \quad h_1 \quad \frac{h_{2s} \quad h_1}{\eta_s} \tag{4}$$

In case of existence of coolant water heat source, output CO_2 temperature is calculated by assuming 15 °C temperature differences between coolant and CO_2 streams. Then by applying energy balance on the heat exchanger first possible CO_2 mass flow rate could be calculated as:

$$\dot{m}_{1,\,CO_2} \quad \dot{m}_w c_{p,w} \frac{T_{wi} \quad T_{wo}}{h_3 \quad h_2} \tag{5}$$

By assuming 15 °C temperature differences between exhaust gases and inlet expander temperature ($T_{exi} - T_5 = 15$) and knowing expander inlet and outlet pressure and the expander efficiency, the next step is to compute the outlet expander enthalpy (then temperature) by employing the equation:

$$h_6 = h_4 - \eta_{exp}(h_5 - h_{6s}) \tag{6}$$

The internal heat exchanger calculation requires more efforts. As the temperature change in the heat exchanger is quite high, instead of employing traditional way of assuming constant specific heat and working with temperature difference (*e. g.* LMTD or ε-NTU) the enthalpy has been used to figure out heat exchange in the internal heat exchange as:

$$q \quad \frac{\dot{Q}}{\dot{m}_{CO_2}} \quad h_4 \quad h_3 \quad h_6 \quad h_7 \tag{7}$$

The maximum heat exchange in the heat exchanger is occurred when either T_7 approaches T_3 or T_4 approaches T_6 and could be calculated as:

$$q_{\max} \quad \min.(q_1, q_2) \quad \text{when} \quad \begin{matrix} q_1 & h_{4(T_4 \ T_6)} & h_3 \text{ when } T_4 \text{ approaches } T_6 \\ q_2 & h_6 & h_{7(T_7 \ T_3)} \text{ when } T_7 \text{ approaches } T_3 \end{matrix} \tag{8}$$

Once the maximum heat exchange is found, the outlet enthalpies of the heat exchanger (then temperatures) could be found by assuming a value for heat exchanger effectiveness and employing the equations:

$$h_4 = h_3 + \varepsilon q_{\max} \tag{9}$$

$$h_7 = h_6 + \varepsilon q_{\max} \tag{10}$$

Considering gas heat source in next step, output CO_2 and exhaust gases temperature are fixed by 15 °C temperature differences between exhaust gases and CO_2 streams ($T_{\text{exi}} - T_5 = 15$ and $T_{\text{exo}} - T_4 = 15$). Then by applying energy balance on the gas heater heat exchanger, the second possible CO_2 mass flow rate could be calculated as:

$$\dot{m}_{2,\,CO_2} \quad \dot{m}_{\text{ex}} c_{\text{p, ex}} \frac{T_{\text{exi}} \quad T_{\text{exo}}}{h_4 \quad h_3} \tag{11}$$

To prevent violation of second law of thermodynamic in gas or water heat source, the correct mass flow rate of the CO_2 stream is calculated as:

$$\dot{m}_{CO_2} \quad \min.(\dot{m}_{1,\,CO_2}, \dot{m}_{2,\,CO_2}) \tag{12}$$

Once the correct CO_2 mass flow rate is calculated, the condition of CO_2 stream and exhaust gas at exit of water and gas heat sources are recalculated.

Now it would be possible to compute the pump input power, the expander and net output power and the cycle thermal efficiency as:

$$\dot{W}_{\text{p}} \quad \dot{m}_{CO_2}(h_2 \quad h_1) \tag{13}$$

$$\dot{W}_{\text{exp}} \quad \dot{m}_{CO_2}(h_6 \quad h_7) \tag{14}$$

$$\dot{W}_{\text{net}} \quad \dot{W}_{\text{exp}} \quad \dot{W}_{\text{p}} \tag{15}$$

$$\eta_{th} \quad \frac{\dot{W}_{\text{net}}}{\dot{m}_{CO_2}(h_5 \quad h_4 \quad h_3 \quad h_2)} \tag{16}$$

It is interested to note that the cycle thermal efficiency is not depended upon CO_2 mass flow rate.

Results and discussion

Cycle with gas heat source (GHC)

A schematic diagram of a CO_2 transcritical power cycle with gas heat source is shown in fig. 5. In this case all heat input to the CO_2 power cycle is supplied through the engine exhaust

gases. As a result, the maximum cycle temperature (expander inlet temperature) would be dependent upon exhaust gas temperature.

Figure 9 shows the potential mass flow rate of CO_2 within the power cycle for pressure ratio of 2. It should be pointed out that the results for various pressure ratio show that the pressure ratio has very small effect on potential mass of CO_2 flow rate. As it can be seen the CO_2 mass flow rate increases as engine speed increases and follow nearly a line. The mass flow rate for full engine load are higher than half load and their difference increases as engine speed increases. Knowing the CO_2 mass flow rate would be necessary for sizing components and especially for designing the pump (*e. g.* the characteristic curve of pump should follow same trends as in fig. 9 to meet the CO_2 mass flow rate demand).

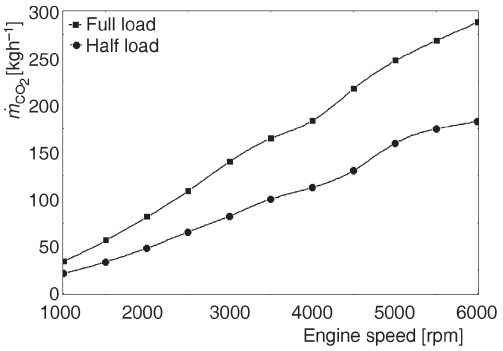

Figure 9. Potential CO_2 cycle mass flow rate *vs.* engine speed

Figure 10 presents the net power output of the CO_2 cycle. The effect of pressure ratio has been also shown. The net output power is ranging from 1 to 6 kW at half engine load and from 1.2 to 8 kW at full engine load for pressure ratio of 2. Note from the figure, as pressure ratio increases, the net output power increases too. The pressure ratio has bigger effect in higher engine speed than lower engine speed. As expected, the maximum power is generated by the CO_2 power cycle at pressure ratio of 5. In this case, as much as 15 kW of power could be generated at highest engine speed and load. This is considerable amount of power if compared with maximum engine brake power (80 kW).

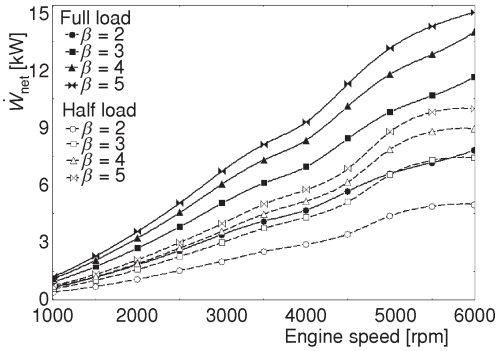

Figure 10. Effect of pressure ratio on CO_2 cycle net output power in various engine speeds

Cycle with gas and water heat sources (GWHC)

A schematic diagram of a CO_2 transcritical power cycle with gas and water heat sources is shown in fig. 6. Again, the maximum cycle temperature (expander inlet temperature) would be depended upon exhaust gas temperature in this case too.

Figure 11 displays the potential mass flow rate of CO_2 within the cycle for pressure ratio of 2. The same conclusions as in the previous case

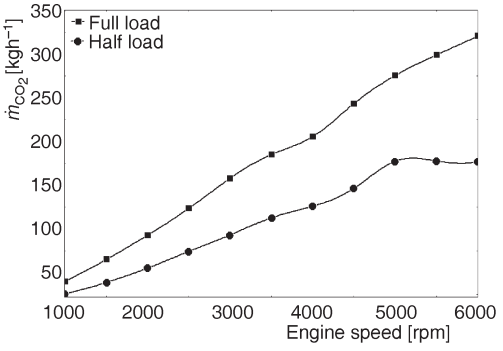

Figure 11. Potential CO_2 cycle mass flow rate *vs.* engine speed

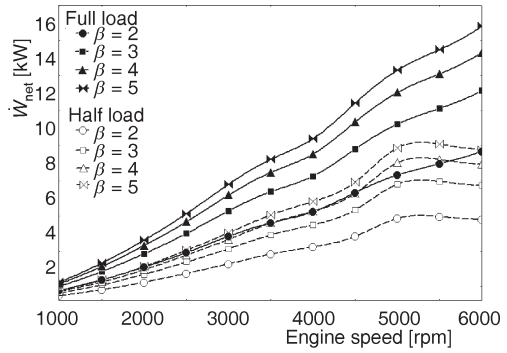

Figure 12. Effect of pressure ratio on CO_2 cycle net output power in various engine speeds

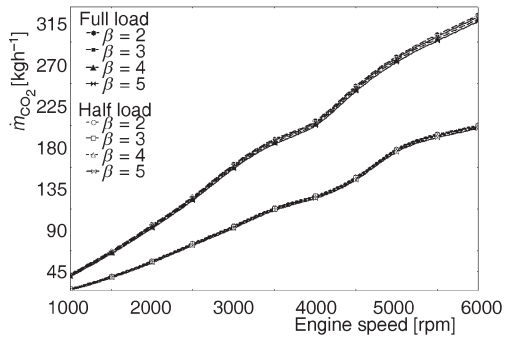

Figure 13. Potential CO_2 cycle mass flow rate *vs.* engine speed

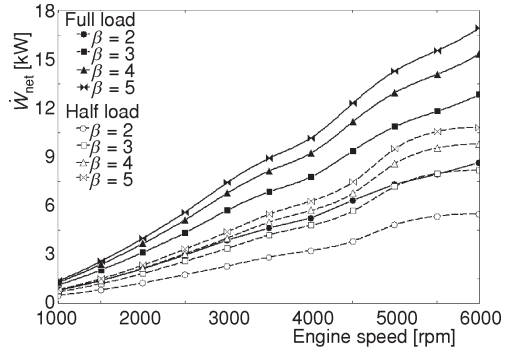

Figure 14. Effect of pressure ratio on CO_2 cycle net output power in various engine speeds

could be made except the fact that for this case, the CO_2 mass flow rate is higher than previous one.

Figure 12 presents the net power output of the CO_2 cycle for this case. The effect of pressure ratio has been also shown. The same conclusions as in the previous case could be made except the fact that for this case the net output power increases slightly. The amount of power increase may not be high enough to add a water heat source to the cycle.

Cycle with gas heat sources and internal heat exchanger (GHIC)

A schematic diagram of a CO_2 transcritical power cycle with gas heat source and internal heat exchanger is shown in fig. 7. Again, the maximum cycle temperature (expander inlet temperature) would be depended upon exhaust gas temperature in this case too.

Figure 13 displays the potential mass flow rate of CO_2 within the cycle for various engine speeds. The effects of pressure ratio on the potential mass flow rate can also be investigated. The same conclusions as in the previous cases could be made. In addition it could be realized that pressure ratio has small effect on the cycle mass flow rate.

Figure 14 shows the net power output of the CO_2 cycle for this case. The effect of pressure ratio has been also shown. The same conclusions as in the previous cases could be made except the fact that for this case the net output power increases slightly comparing to previous cases.

Cycle with gas and water heat sources with internal heat exchanger (GWHIC)

A schematic diagram of a CO_2 transcritical power cycle with gas and water heat sources and internal heat exchanger is shown in fig. 8. Again, the maximum cycle temperature (expander inlet temperature) would be depended upon exhaust gas temperature in this case too.

Figure 15 shows the potential mass flow rate of CO_2 within the cycle for various engine speeds. The effects of pressure ratio on the potential mass flow rate can also be investigated. The same conclusions as the previous cases could be made. In addition it could be realized that pressure ratio has bigger effect on the cycle mass flow rate compared with previous cases.

Figure 16 shows the net power output of the CO_2 cycle for this case. The effect of pressure ratio can also be investigated in the figure. The same conclusions as the previous cases could be made except the fact that for this case the net output power reaches almost 18 kW at full engine load and speed. This is considerable amount of power if compared with maximum engine brake power which is 80 kW.

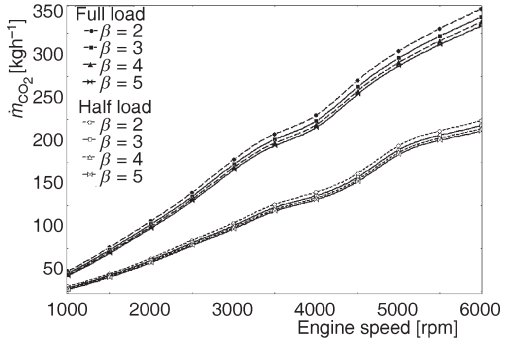

Figure 15. Potential CO_2 cycle mass flow rate *vs.* engine speed

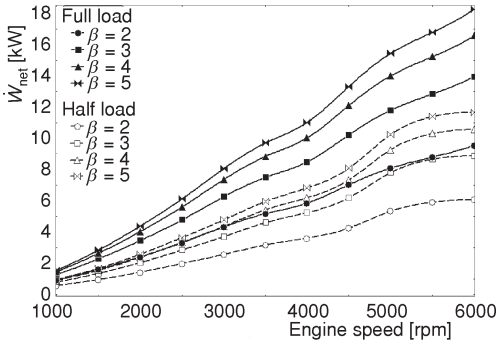

Figure 16. Effect of pressure ratio on CO_2 cycle net output power in various engine speeds

Once the hear recovery power cycle has been utilized, a part of heat will converted to power. Figure 17 shows the new energy balance for the case where $\beta = 3$. It could be realized that about 5% of fuel energy is converted to power by CO_2 power cycle for all engine speed.

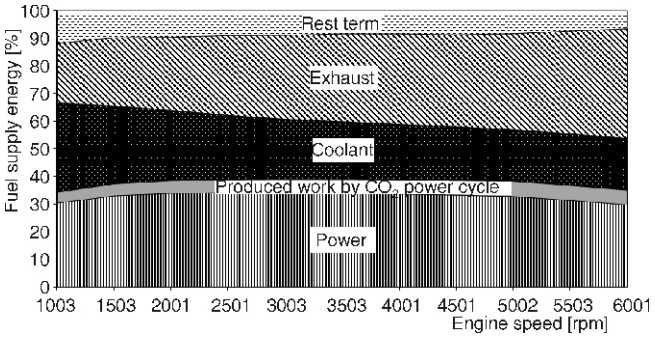

Figure 17. The energy balance at full load for various engine speeds after utilizing CO_2 power cycle where $\beta = 3$

Comparison among configurations

Before comparing results for various cycle configurations, it would be instructive to plot *T-s* diagram for one case. Figure 18 shows the *T-s* diagram for GWHIC configuration at full engine load and speed for pressure ration of 2. It could be realized that CO_2 stream is at superheat conditions for most of cycle except at heat sink (the condenser) and partly at water heat source. The heat source pressure is above critical pressure. For GHIC configuration, the CO_2 stream in internal heat exchanger travels near the critical point. In this case, the traditional heat exchange calculation methods would not give accurate results.

Figure 19 shows the potential mass flow rate of CO_2 for all configurations and $\beta = 3$ *vs.* engine speed. It can be easily realized that the CO_2 mass flow rate in GWHIC configuration is highest flow rate among all configurations. This is due to the fact that in GWHIC case, there are 2 heat sources with one internal heat exchanger, this supplies highest heat to the cycle. The lowest the CO_2 mass flow rate belongs to GHC configurations which only have one heat source.

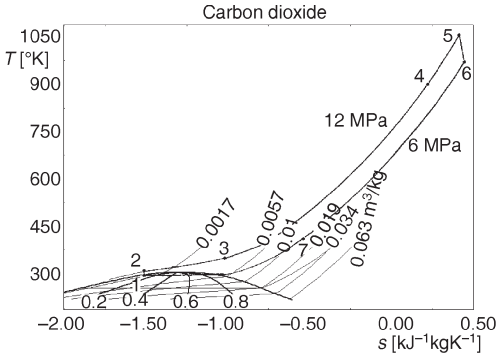

Figure 18. *T-s* diagram for GWHIC configuration at engine speed of 6000 rpm and $\beta = 2$ for full engine load

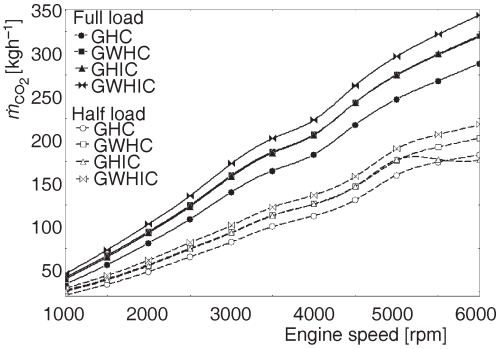

Figure 19. Comparing potential CO_2 cycle mass flow rate at full and half engine load for $\beta = 3$

Figure 20 compares the net power output for all configurations for half and full engine load. It could be realized that the net power increases slightly as the configurations gets more components so one may conclude that it may not be worth to add more components to simplest configuration as GHC.

Figure 21 compares the thermal efficiency for all configurations when $\beta = 3$ and for full engine load. It could be realized that the GHIC has highest thermal efficiency. The other configuration with internal heat exchanger has (IHX) second highest thermal efficiency. Then there is a huge drop in thermal efficiency for configuration without IHX. The reason behind it is that, for configuration with IHX, part of heat supply to the cycle comes through the IHX itself. If the IHX

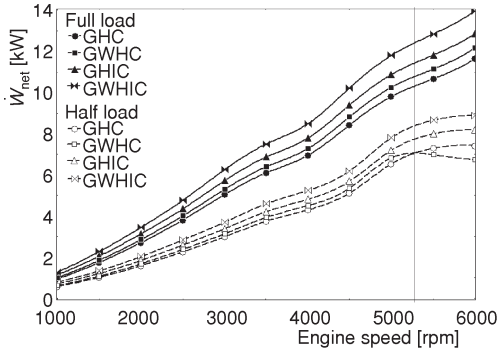

Figure 20. Comparing net output power at full and half engine load for $\beta = 3$

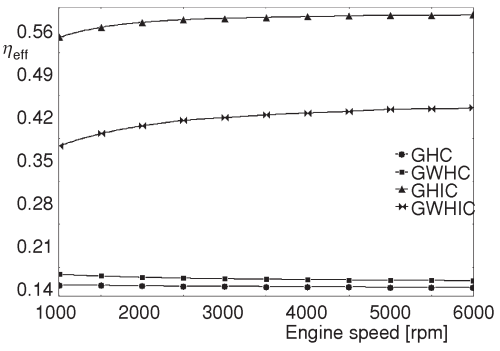

Figure 21. Comparing thermal efficiency of all configurations at full engine load for $\beta = 3$

does not exist in the cycle, the heat has to be rejected in the heat sink. This makes the cycles without IHX to have much lower thermal efficiency.

Despite the fact that the cycles with IHX have much higher thermal efficiency, but as the net output power is slightly higher for these cases, one may conclude that add an IHX to the cycle is worth only when another simultaneous heat recovery system exists.

Conclusions

It is well known that majority of fuel energy in a typical engine are wasted through exhaust gases and cooling water radiator. These make exhaust and cooling water heat recovery is matter of necessary in current world energy situation. Various methods have been proposed to recover energy from an ICE waste heat to produce power or refrigeration. One of the attractive waste energy recovery methods is CO_2 gas power cycle. The method has the potentials to be implemented in a typical car to convert heat lost to usable work.

The present work provides details about energy accounting of a natural gas powered ICE and achievable work of a utilized CO_2 power cycle. Based on experimental performance analysis of a new designed IKCO (Iran Khodro Company) 1.7 liter natural gas powered ICE, full energy accounting of the engine was carried out on various engine speeds and loads. The energy accounting includes (a) exhaust gases analysis, its temperature, and mass flow rate, (b) coolant inlet and outlet temperature and its mass flow rate, and (c) the engine brake power and torque. The results show that coolant water and exhaust gases heat lost are destroyed about 60% of input fuel energy at various engine speeds and loads. The coolant water destroyed more energy in lower engine speed and exhaust gases waste more energy in higher engine speed.

Further, 4 CO_2 transcritical power cycle configurations have been appointed to take advantages of exhaust and coolant water heat lost. Based on thermodynamic analysis, a calculation method has been developed to study these cycles. Based on the method, the amount of recoverable work has been calculated on various engine conditions. The results show that one can generate as much as 18 kW of power by employing power cycle. The results also indicated that, take advantage of coolant water heat sources and employing IHX would raise net output power slightly which may not be high enough to add more components to the cycles. The additional components are worth to add only when another simultaneous heat recovery system exists.

Acknowledgments

This work was supported by research grant from Shahrood University of Technology.

Nomenclature

- c_p – constant pressure specific heat, [kJkg^{-1}K^{-1}]
- h – specific enthalpy, [kJkg^{-1}]
- LHV – lower heating value, [MJkg^{-1}]
- $\dot{m}$ – mass flow rate, [kgs^{-1}]
- $\dot{m}_{ex}$ – mass flow rate of exhaust gas, [kgs^{-1}, kgh^{-1}]
- $\dot{m}_w$ – cooling water flow are at radiator, [kgs^{-1}, kgh^{-1}]
- $\dot{Q}$ – heat transfer rate, [kW]
- $\dot{Q}_{ex}$ – exhaust gas heat transfer, [kW]
- $\dot{Q}_w$ – coolant heat lost, [kW]
- q_{max} – maximum heat transfer in heat exchanger, [kJkg^{-1}]
- T – temperature, [K]
- T_{exi} – temperature of exhaust manifolds after catalyst, [K]
- T_{exo} – temperature of exhaust manifolds before catalyst, [K]

T_{wi} – cooling water temperature on radiator inlet, [K]
T_{wo} – cooling water temperature on radiator outlet, [K]
T_{ex1} – temperature of exhaust runner No. 1, [K]
T_{ex2} – temperature of exhaust runner No. 2, [K]
T_{ex3} – temperature of exhaust runner No. 3, [K]
T_{ex4} – temperature of exhaust runner No. 4, [K]
T_0 – ambient temperature, [K]
$\dot{W}$ – power, [kW]
$\dot{W}_{exp}$ – expansion output power, [kW]
$\dot{W}_{net}$ – net cycle power, [kW]
$\dot{W}_p$ – pump input power, [kW]

Greek letters

β – pressure ratio, [–]
ε – heat exchanger effectiveness, [–]
η – efficiency, [–]
η_p – pump isentropic efficiency, [–]
η_{th} – the cycle thermal efficiency, [–]

Subscript

ex – exhaust gas
exi – inlet exhaust gas at gas heat source
exo – outlet exhaust gas at gas heat source
exp – expander
f – fuel
mix – mixture of exhaust gases
p – pump
res – rest term
s – isentropic
th – thermal
w – water
wi – inlet water at water heat source
wo – outlet water at water heat source
0 – ambient

Acronimes

GHC – cycle with gas heat source
GHIC – cycle with gas heat source & internal heat exchanger
GWHC – cycle with gas and water heat sources
GWHIC – cycle with gas & water heat sources and internal heat exchanger
ICE – internal combustion engine
IHX – internal heat exchanger
IKCO – Iran Khodro Company
SI – spark ignition

References

[1] Ravikumar N., Ramakrishna K., Sitaramaraju A. V., Thermodynamic Analysis of Heat Recovery Steam Generator in Combined Cycle Power Plant, *Thermal Science, 11* (2007), 4, pp. 143-156
[2] Polyzakis, A. L., *et al*., Long-Term Opitimisation Case Studies for Combined Heat and Power System, *Thermal Science, 13* (2009), 4, pp. 46-60
[3] Chen, Y., Novel Cycles Using Carbon Dioxide as Working Fluid, Ph. D. thesis, Division of Applied Thermodynamics and Refrigeration, Energy Department, KTH University, Stockholm, 2006
[4] Dostal, V., *et al.*, Supercritical CO_2 Cycle for Fast Gas Cooled Reactors, *Proceedings on CD*, ASME Turbo Expo, Power for Land, Sea and Air, Vienna, paper GT2004-54242, 2004
[5] Chen, Y., Lundqvist, P., Platell, P., Theoretical Research of Carbon Dioxide Power Cycle Application in Automobile Industry to Reduce Vehicles Fuel Consumption, *Applied Thermal Engineering, 25* (2005), pp. 14-15, 2041-2053, doi:10.1016/j.applthermaleng.2005.02.001
[6] Farzaneh-Gord, M., *et al*., Estimating Recoverable Work of an Engine by Utilizing the CO_2 Brayton Power Cycle and Capturing Heat Lost, *Archives of Thermodynamics, 30* (2009), 3, pp. 1-22
[7] Farzaneh-Gord, M., *et al*., Simulation of CO_2 Power Cycle and Theoretical Investigation of Its Application in Internal Combustion Engine, *Proceedings on CD*, 3rd International Conference on Modelling, Simulation and Applied Optimization, Sharjah, UAE, 2009
[8] Cayer, E., *et al*., Analysis of a Carbon Dioxide Transcritical Power Cycle Using a Low Temperature Source, *Appl Energy* (2008), doi:10.1016/j.apenergy.2008.09.018
[9] Brown, J. S., Yana-Motta, S. F., Domanski, P. A. Comparitive Analysis of an Automotive Air Conditioning Systems Operating with CO_2 and R134a, *International Journal of Refrigeration, 25* (2002), 1, pp. 19-32
[10] Ramanathan, A., Gunasekaran, P., Simulation of Absorption Refrigeration System for Automobile Application, *Thermal Science, 12* (2008), 3, pp. 5-13
[11] Farzaneh-Gord, M., Maghrebi, M. J., Hajializadeh, H., Optimizing Four Stroke Spark Ignition Engine Performance, Proceeding, The 2nd International Conference on Modeling, Simulation, and Applied Optimization, Abu Dhabi, UAE, 2007

[12] Evans, R. L., Jarmer, D. R., Experimental Validation of an Engine Simulation Code with Lean-Burn Natural Gas Engine Data , SAE technical paper series 981909, 1998
[13] Stone, R., Introduction to Internal Combustion Engines, Department of Engineering Science, University of Oxford, Oxford, UK, 1999
[14] Rakopoulos, C. D., Kyritsis, D. C., Comparative Second-Law Analysis of Internal Combustion Engine Operation for Methane, Methanol, and Dodecane Fuels, *Energy, 26* (2001), 7, pp. 705-722, doi:10.1016/S0360-5442(01)00027-5
[15] Sobiesiak, A., Zhang, S., The First and Second Law Analysis of Spark Ignition Engine Fuelled with Compressed Natural Gas, SAE International, 2003-01-3091

Paper submitted: March 1, 2009
Paper revised: September 11, 2009
Paper accepted: February 14, 2010